

# Strongly quadrature-dependent noise in superconducting micro-resonators measured at the vacuum-noise limit

J. Gao, L. R. Vale, J. A. B. Mates, D. R. Schmidt, G. C. Hilton, and K. D. Irwin

*National Institute of Standards and Technology, Boulder, CO 80305-3337*

F. Mallet, M. A. Castellanos-Beltran, and K. W. Lehnert

*JILA and the Department of Physics,*

*National Institute of Standards and Technology and*

*University of Colorado, Boulder, CO 80309-0440*

J. Zmuidzinas and H. G. Leduc

*Jet Propulsion Laboratory, California Institute of Technology, Pasadena, CA 91125*

(Dated: August 26, 2018)

## Abstract

We measure frequency- and dissipation-quadrature noise in superconducting lithographed microwave resonators with sensitivity near the vacuum noise level using a Josephson parametric amplifier. At an excitation power of 100 nW, these resonators show significant frequency noise caused by two-level systems. No excess dissipation-quadrature noise (above the vacuum noise) is observed to our measurement sensitivity. These measurements demonstrate that the excess dissipation-quadrature noise is negligible compared to vacuum fluctuations, at typical readout powers used in micro-resonator applications. Our results have important implications for resonant readout of various devices such as detectors, qubits and nano-mechanical oscillators.

Superconducting lithographed microwave resonators (micro-resonators) are used in a broad range of applications, such as photon detection[1], readout of superconducting quantum interference devices (SQUIDs)[2], measurement of qubits[3] and detection of nanomechanical motion[4]. In these applications, the sensing element presents a variable reactive or dissipative load to the micro-resonator. The microwave probe signal, transmitted through or reflected from the resonator, is sensitive to changes in resonance frequency  $f_r$  in one quadrature of the microwave field (referred to as the frequency quadrature,  $\hat{\xi}_{\parallel}$  in Fig. 1), and changes in quality factor  $Q_r$  (or internal dissipation) in the orthogonal quadrature (referred to as the dissipation quadrature,  $\hat{\xi}_{\perp}$  in Fig. 1). The use of these two quadratures is often referred to as frequency readout and dissipation readout, respectively.

The sensitivity of these measurements may be limited by the noise in the microwave probe signal, the intrinsic noise of the resonator, and noise in the readout electronics, usually set by the noise temperature  $T_n$  of the amplifier. These noise contributions can also be projected into the two quadratures, with power spectra  $S_{\parallel}$  and  $S_{\perp}$  for  $\hat{\xi}_{\parallel}$  and  $\hat{\xi}_{\perp}$ , respectively. In general, the noise power can be quadrature-dependent;  $S_{\parallel} \neq S_{\perp}$ . If both the resonator and the amplifier have no excess noise, the ultimate sensitivity will be limited quantum mechanically by the vacuum noise, which is a quarter photon per quadrature ( $S_{\parallel} = S_{\perp} = hf/4$ ).

We have previously reported that at high excitation power significant excess noise in the frequency quadrature is universally observed in superconducting micro-resonators and suggested that a surface layer of two-level system (TLS) fluctuators are responsible for this noise[5, 6]. In contrast, no excess noise in the dissipation quadrature was observed above the noise floor of a high electron mobility transistor (HEMT) amplifier. However, a state-of-the-art HEMT has  $T_n \approx 5$  K at 6 GHz, which is 35 times the vacuum noise. Therefore, it has been unclear whether micro-resonators produce excess noise in the dissipation quadrature above the vacuum noise level. On the other hand, microwave amplifiers based on SQUIDs, including dc-SQUID amplifiers[7, 8] and Josephson parametric amplifiers (JPA)[9], have recently demonstrated nearly ideal performance. For example, our group has demonstrated a JPA that is tunable between 4-8 GHz and adds only 0.3 photon of noise[10]. It is possible, and indeed promising to use these quantum amplifiers to improve the sensitivity of resonator dissipation measurements, provided that the excess noise in the dissipation quadrature of the resonator is well below the HEMT noise floor.

In this Letter, we report the measurement of the resonator noise using a Josephson parametric amplifier. We have achieved a system noise floor as low as 1.8 times the vacuum noise or a factor of 23 lower than a HEMT by using the JPA as a nearly noiseless preamplifier. These measurements, for the first time, show that the excess resonator noise in the dissipation quadrature can be below the vacuum noise, at an excitation power that is appropriate for kinetic inductance detector(MKID)[1] readout.

We measured the noise of a quarter-wave coplanar waveguide (CPW) resonator, made by patterning a 200 nm-thick Nb film deposited on a high-purity intrinsic silicon ( $15 \text{ k}\Omega \cdot \text{cm}$ ) substrate. The CPW resonator has a center strip width of  $5 \mu\text{m}$ , gaps of  $1 \mu\text{m}$ , and is capacitively coupled to a CPW feedline (see Fig. 1(a)). From the transmission  $S_{21}$  data, we have determined  $f_r = 6.23 \text{ GHz}$  and  $Q_r = 1.5 \times 10^5$  (internal  $Q_i = 9 \times 10^5$ ).

Another crucial component for this experiment is a Josephson parametric amplifier, which uses the nonlinear inductance of a Josephson junction to achieve parametric amplification[9]. The JPA used in this experiment consists of a Nb on Si quarter-wave CPW resonator whose center conductor is terminated by an array of 10 SQUIDs in series. A schematic of the JPA and a microscope picture of the SQUIDs are shown in Fig. 2. Here we use a parallel gradiometric SQUID design to minimize the magnetic noise pick-up. A flux-bias line with a built-in RF-choke is used to tune the center frequency of the JPA.

We connect the resonator to the JPA in a configuration shown in Fig. 3. Four microwave signals with phase and/or amplitude control are generated: a resonator excitation tone  $A_e$  to excite the resonator, a carrier suppression tone  $A_s$  to cancel the coherent carrier ( $A_e S_{21}$ ) in the transmitted signal, a pump tone  $A_p$  to pump the JPA, and a calibration tone  $A_{\text{cal}}$  that is always detuned from  $A_e$  by 100 kHz, to calibrate the noise measurement. The three tones  $A_s$ ,  $A_p$  and  $A_{\text{cal}}$  are injected through a directional coupler between the resonator and the JPA. After carrier suppression, only the resonator noise signal is sent to the JPA for amplification, which prevents the JPA from saturating and also allows the phase of  $A_p$  to be independently adjusted relative to the noise signal. The resonator and JPA, along with other components inside the dashed rectangle in Fig. 3, are cooled in an adiabatic demagnetization refrigerator (ADR) to 100 mK.

We first characterize our JPA by turning off the  $A_e$  and  $A_s$  tones. When  $A_p$  is also turned off and no flux bias is applied, the JPA shows a resonance frequency of  $f_{\text{JPA}} = 6.80 \text{ GHz}$  and  $Q_{\text{JPA}} \sim 150$  (coupling-limited). With flux bias,  $f_{\text{JPA}}$  is tunable between 5.8 GHz and

6.80 GHz while  $Q_{\text{JPA}}$  remains constant. When  $A_p$  is turned on, the JPA gives a power gain  $0 \leq G \leq 35$  dB and an amplitude gain-bandwidth product of 45 MHz[10]. The highest gain occurs at a critical pump power  $P_c \approx -93$  dBm (500 fW). Above  $P_c$ , the JPA response is bistable[11].

We then turn off  $A_p$  and detune the JPA frequency  $f_{\text{JPA}}$  far from the resonator's frequency  $f_r$ . This allows us to measure the resonator noise directly with the HEMT. The noise spectra  $S_{\parallel}$  and  $S_{\perp}$  measured at an excitation (internal) power[5]  $P_{\text{int}} \approx -40$  dBm (100 nW) are plotted in Fig. 4(a) in units of vacuum noise  $\zeta$  ( $\zeta = 1$  corresponds to vacuum noise level). In the frequency quadrature,  $S_{\parallel}$  rises well above the HEMT noise floor and the level is consistent with that reported in Ref. [5]. In the dissipation quadrature, no excess noise is seen above the HEMT noise floor. This HEMT noise referred to the input port of the JPA is found to be  $\zeta = 40$  or  $T_n = 6$  K.

To reveal the actual resonator noise in the dissipation quadrature, we use the JPA as a preamplifier before the HEMT. We first operate the JPA in the “nondegenerate” mode by detuning  $A_p$  (generated by a second synthesizer) from both  $A_e$  and  $A_s$  by 2.3 MHz. In this mode, the JPA is a linear phase-insensitive amplifier that amplifies both quadratures with a power gain chosen to be  $G = 16$ . The results are shown in Fig. 4(b). In the frequency quadrature,  $S_{\parallel}$  matches that directly measured by the HEMT (the cyan line). In the dissipation quadrature, except for a  $1/f$  noise below 10 Hz, no excess noise is seen above the system noise floor (the black line). With  $G = 16$ , the JPA achieves a system noise of  $\zeta = 5.1$ , a factor of 8 better than the HEMT (dashed line). Out of the  $\zeta = 5.1$  system noise, the HEMT contributes  $\zeta = 2.5$  ( $40/16$ ), vacuum and thermal noise contributes  $\zeta = 1.3$ , and our JPA adds  $\zeta = 1.3$ . According to the quantum theory of amplifiers[13], a linear phase-insensitive amplifier must add noise at least as large as the vacuum ( $\zeta = 1$ ), which is called the standard quantum limit (SQL). We infer that the JPA itself has in fact added only  $\zeta = 0.3$  noise above the SQL. By operating at higher gain this JPA should be able to achieve a system noise as low as  $\zeta = 1.3$ [14].

Next, we measure the resonator noise with the JPA operating in the “degenerate” mode. In this mode, all the tones are generated by the same synthesizer at the same frequency, which minimizes the effect of synthesizer phase noise. The JPA in the degenerate mode is a phase-sensitive amplifier that amplifies a specific quadrature  $\hat{a}$  of the input signal by a factor of  $\sqrt{G}$  and squeezes (deamplifies) its orthogonal quadrature  $\hat{s}$  by the same factor. In

this measurement, we carefully align the resonator dissipation quadrature  $\hat{\xi}_\perp$  to the JPA amplification quadrature  $\hat{a}$  (see Fig. 4(e)). With adequate gain ( $G \gtrsim 40$ ), the vacuum noise or any excess noise in the dissipation quadrature is amplified and visible above the HEMT noise floor (dashed pink circle). A power gain of  $G \sim 100$  is used. To accurately align  $\hat{\xi}_\perp$  with  $\hat{a}$ , we adjust the phase of  $A_p$  with respect to the input resonator noise signal. When  $\hat{\xi}_\perp$  and  $\hat{a}$  are misaligned by an angle  $\theta$ , the output spectrum for the amplified quadrature  $\hat{a}$  is  $S_{aa}^{\text{out}} = G(S_\perp \cos^2 \theta + S_\parallel \sin^2 \theta)$ . Because we know  $S_\parallel \gg S_\perp$ ,  $S_{aa}^{\text{out}}/G \geq S_\perp$  and the minimum occurs when  $\hat{\xi}_\perp$  and  $\hat{a}$  are perfectly aligned ( $\theta = 0$ ). The red line in Fig. 4(c) shows the lowest measured noise spectrum from the amplified quadrature of the JPA referred to noise in the resonators. Again, we see no excess noise above the system noise floor (black line). The system noise (white noise above 10 kHz) corresponds to  $\zeta = 1.8$  (a factor of 23 lower than the HEMT), with the HEMT accounting for  $\zeta = 0.4$  (40/100), vacuum and thermal noise accounting for  $\zeta = 1.3$ , and the JPA adding  $\zeta = 0.1$ . According to the quantum theory of amplifiers, there is no SQL for the noise added by an amplifier that amplifies only one quadrature. Indeed, for modulation frequencies about 10 kHz, our JPA is almost noiseless when operating at high gain in the degenerate mode. However, we do see in Fig. 4(c) substantial noise below 10 kHz. We find that the noise level and shape changes when  $f_{\text{JPA}}$  is tuned away from  $f_r$ . We suspect that the pump tone can excite the resonator and add noise even when  $A_e$  is off, due to the finite directivity (-40 dB total) of the circulators.

The results of the noise measurements made using the HEMT, and using the JPA in the nondegenerate and degenerate modes, are combined in Fig. 4(d), where the red line plots the lowest measured  $S_\perp$  at each frequency. The excess resonator noise in the dissipation quadrature is constrained by this noise line. Because this noise line contains other noise contributions (HEMT, vacuum and thermal noise), we can further tighten this constraint by subtracting the system noise floor from the measured noise level. This yields the gray line in Fig. 4(d), which reaches below the vacuum noise (the dotted line) at  $\nu > 100$  Hz. Therefore, the excess resonator noise in the dissipation quadrature is constrained to lie below the vacuum noise at modulation frequencies above 100 Hz, which is the main conclusion of this letter.

The property that the resonator noise is entirely directed in the frequency quadrature, with  $S_\parallel$  rising orders of magnitude above and  $S_\perp$  remaining below the vacuum noise, is an extremely interesting observation. Previous studies, including the power[5],

temperature[15], and geometry dependence[6] of the frequency noise, its origin in the resonator capacitance[16], and the anomalous frequency shift below 1 K[17], have led to a consistent picture in which the noise is caused by a surface layer of TLS fluctuators in the dielectric materials. In this picture, TLS saturation plays an important role. Indeed, the average response  $\chi(\omega)$ [6] of a TLS to the microwave field  $|\vec{E}|$  is given by[18]

$$\chi(\omega) \propto \frac{\omega_0 - \omega}{(\omega_0 - \omega)^2 + (s/T_2)^2} + j \frac{T_2^{-1}}{(\omega_0 - \omega)^2 + (s/T_2)^2},$$

where  $\omega_0$  is the transition frequency of the TLS,  $T_2$  is the transverse relaxation time,  $s = [1 + (|\vec{E}|/E_c)^2]^{-1/2}$  is the power broadening factor ( $s \gtrsim 100$  is estimated for our case) and  $E_c$  is a critical electric field[19]. While power-broadening expands the line width by a factor of  $s$ , it also reduces the peak strength of the reactive response by  $s$ , and the dissipative response by  $s^2$ . Therefore the effect on the noise goes as  $s^{-1}$  and  $s^{-3}$ , respectively in the two quadratures. This may qualitatively explain the observed  $P^{-1/2}$  ( $\propto s^{-1}$ ) power dependence of  $S_{\parallel}$  and the large ratio ( $\propto s^2$ ) between  $S_{\parallel}$  and  $S_{\perp}$ . However, although there is some speculation about the TLS noise mechanism[6, 20] and attempts to model this noise [6, 21], so far the physical picture of TLS resonator noise is not well understood and a quantitative model is not available.

In conclusion, we have demonstrated the measurement of resonator noise using a Josephson parametric amplifier. We have achieved a system noise that is 5.1 and 1.8 times the vacuum noise when operating the JPA in nondegenerate and degenerate mode, which is a factor 8 and 23 lower than the HEMT noise. At an excitation power of 100 nW, no excess noise in the dissipation quadrature is observed above the system noise floor. Excess resonator noise in the dissipation quadrature is constrained to be below the vacuum noise above 100 Hz. We suggest that the frequency-only noise property is related to the saturation of two-level systems.

Our results have important implications for resonant readout of sensitive devices. If the sensing element presents a fully or partially resistive load to the resonant circuit and thereby produces a signal in the dissipation quadrature, the use of an ultra-low-noise amplifier (well below the HEMT noise) in a dissipation readout may improve the measurement sensitivity by a large factor. For example, the resonator parameters and excitation power used in this experiment are typical for MKID readout; therefore the sensitivity of MKIDs can be readily improved by a factor of  $\sqrt{23}$  by using the JPA in this letter in degenerate mode, without

requiring modification to the detector design or operating conditions.

We thank Jose Aumentado, Lafe Spietz, John Teufel and John Martinis for useful discussions. The resonator was fabricated in the JPL Microdevices Lab. The JPA was fabricated in the NIST, Boulder fabrication facility. This work was supported in part by the DARPA QUEST program.

- 
- [1] P. K. Day, H. G. LeDuc, B. A. Mazin, A. Vayonakis, and J. Zmuidzinas, *Nature* **425**, 817 (2003).
- [2] J. A. B. Mates, G. C. Hilton, K. D. Irwin, L. R. Vale, and K. W. Lehnert, *Appl. Phys. Lett.* **92**, 023514 (2008).
- [3] A. Wallraff, D. I. Schuster, A. Blais, L. Frunzio, R.-S. Huang, J. Majer, S. Kumar, S. M. Girvin, and R. J. Schoelkopf, *Nature* **431**, 162 (2004).
- [4] C. A. Regal, J. D. Teufel, and K. W. Lehnert, *Nature Phys.* **4**, 555 (2008).
- [5] J. Gao, J. Zmuidzinas, B. A. Mazin, P. K. Day, and H. G. LeDuc, *Appl. Phys. Lett.* **90**, 817 (2007).
- [6] J. Gao, M. Daal, J. M. Martinis, A. Vayonakis, J. Zmuidzinas, B. Sadoulet, B. A. Mazin, P. K. Day, and H. G. Leduc, *Appl. Phys. Lett.* **92**, 212504 (2008).
- [7] M. Mück, C. Welzel, and J. Clarke, *Appl. Phys. Lett.* **82**, 3266 (2003).
- [8] L. Spietz, K. Irwin, and J. Aumentado, *Appl. Phys. Lett.* **95**, 092505 (2009).
- [9] B. Yurke, L. R. Corruccini, P. G. Kaminsky, L. W. Rupp, A. D. Smith, A. H. Silver, R. W. Simon, and E. A. Whittaker, *Phys. Rev. A* **39**, 2519 (1989).
- [10] M. A. Castellanos-Beltran, K. D. Irwin, G. C. Hilton, L. R. Vale, and K. W. Lehnert, *Nature Phys.* **4**, 929 (2008).
- [11] I. Siddiqi, R. Vijay, F. Pierre, C. M. Wilson, M. Metcalfe, C. Rigetti, L. Frunzio, and M. H. Devoret, *Phys. Rev. Lett.* **93**, 207002 (2004).
- [12]  $P_c$  depends on the critical current of the junction and  $Q_{JPA}$ , which are unchanged for the two cases at the same temperature of 4K. We measured  $P_{c,4K} = -93.2$  dBm using a VNA in the calibrated LHe probe test.  $A_{cal}$  is generated by the same VNA at 60.0 dB below  $P_{c,4K}$ , therefore,  $P_{cal} = -153.2$  dBm. We use this calibration method due to the lack of cooling power for a hot-cold load measurement in our ADR . The details of this calibration procedure will be published in a separate paper.
- [13] C. M. Caves, *Phys. Rev. D* **26**, 1817 (1982).
- [14] We have simply chosen a 2.3 MHz signal detuning to exclude the pump tone from the 1 MHz noise sampling bandwidth and all our noise plots. Accordingly, we have used a lower JPA gain  $G=16$  which produces a 5 MHz bandwidth (single-sided) to accommodate the signal. It



is possible to improve the system noise by carefully selecting a smaller signal detuning and a higher JPA gain.

- [15] S. Kumar, J. Gao, J. Zmuidzinas, B. A. Mazin, H. G. LeDuc, and P. K. Day, *Appl. Phys. Lett.* **92**, 123503 (2008).
- [16] O. Noroozian, J. Gao, J. Zmuidzinas, H. G. LeDuc, and B. A. Mazin (*AIP*, 2009), vol. 1185, pp. 148–151.
- [17] J. Gao, M. Daal, A. Vayonakis, S. Kumar, J. Zmuidzinas, B. Sadoulet, B. A. Mazin, P. K. Day, and H. G. Leduc, *Appl. Phys. Lett.* **92**, 152505 (2008).
- [18] W. A. Phillips, *J. Low Temp.Phys.* **7**, 351 (1972).
- [19] J. M. Martinis, K. B. Cooper, R. McDermott, M. Steffen, M. Ansmann, K. D. Osborn, K. Cicak, S. Oh, D. P. Pappas, R. W. Simmonds, et al., *Phys. Rev. Lett.* **95**, 210503 (2005).
- [20] C. C. Yu, *J. Low Temp.Phys.* **137**, 251 (2004).
- [21] M. Constantin, C. C. Yu, and J. M. Martinis, *Phys. Rev. B* **79**, 094520 (2009).

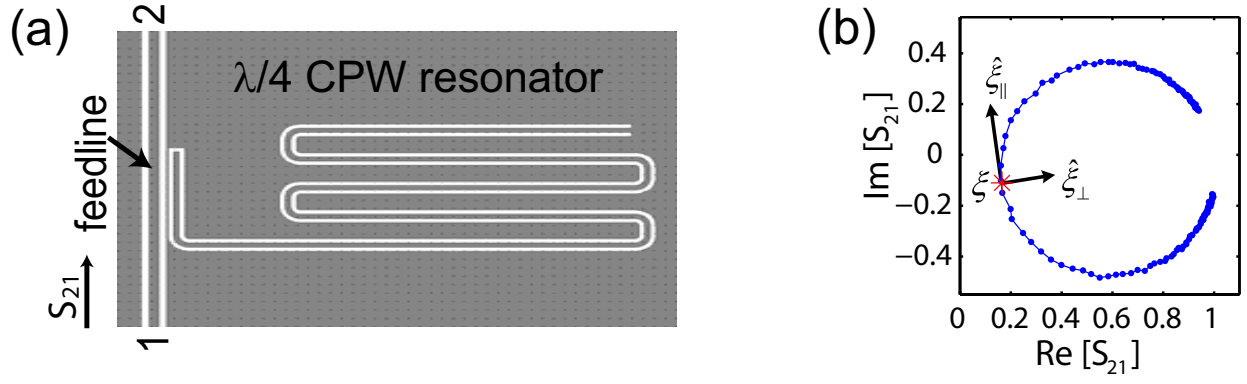


FIG. 1: (a) Schematic illustration (not to scale) of the resonator and feedline (Nb in gray and Si in white). (b) Transmission  $S_{21}$  measured with a vector network analyzer (VNA). A parametric plot of  $\text{Im}[S_{21}(f)]$  vs  $\text{Re}[S_{21}(f)]$  traces out a resonant circle. The resonance point, frequency quadrature (tangential to the circle) and dissipation quadrature (normal to the circle) are indicated by  $\xi$ ,  $\hat{\xi}_{\parallel}$  and  $\hat{\xi}_{\perp}$ , respectively.

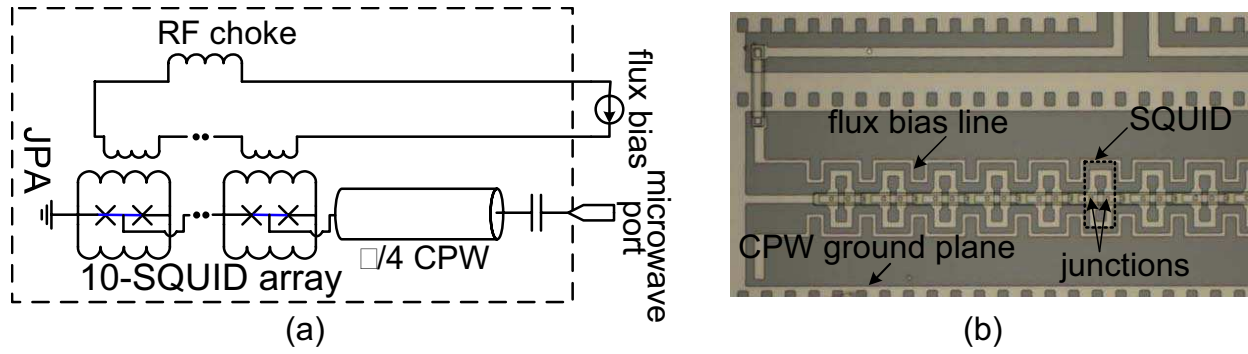


FIG. 2: (a) Schematic of the JPA consisting an array of 10 parallel gradiometric SQUIDs coupled to a flux-bias line. (b) Microscope picture showing the SQUID array.

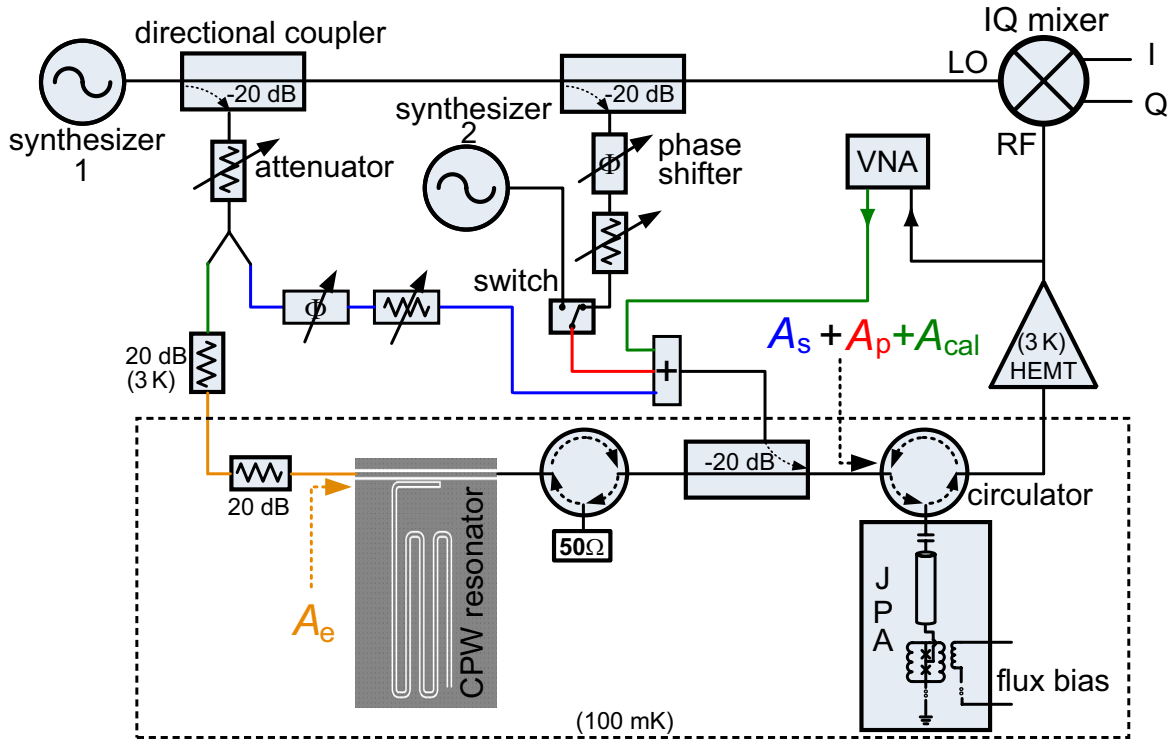


FIG. 3: A diagram of noise measurement setup. The calibration tone  $A_{cal}$  is generated by the VNA that is also used for  $S_{21}$  measurement. A switch is used to select the source of the pump tone between synthesizer 1 and synthesizer 2, which allows the JPA to operate in degenerate mode (switch to the right) or nondegenerate mode (switch to the left).

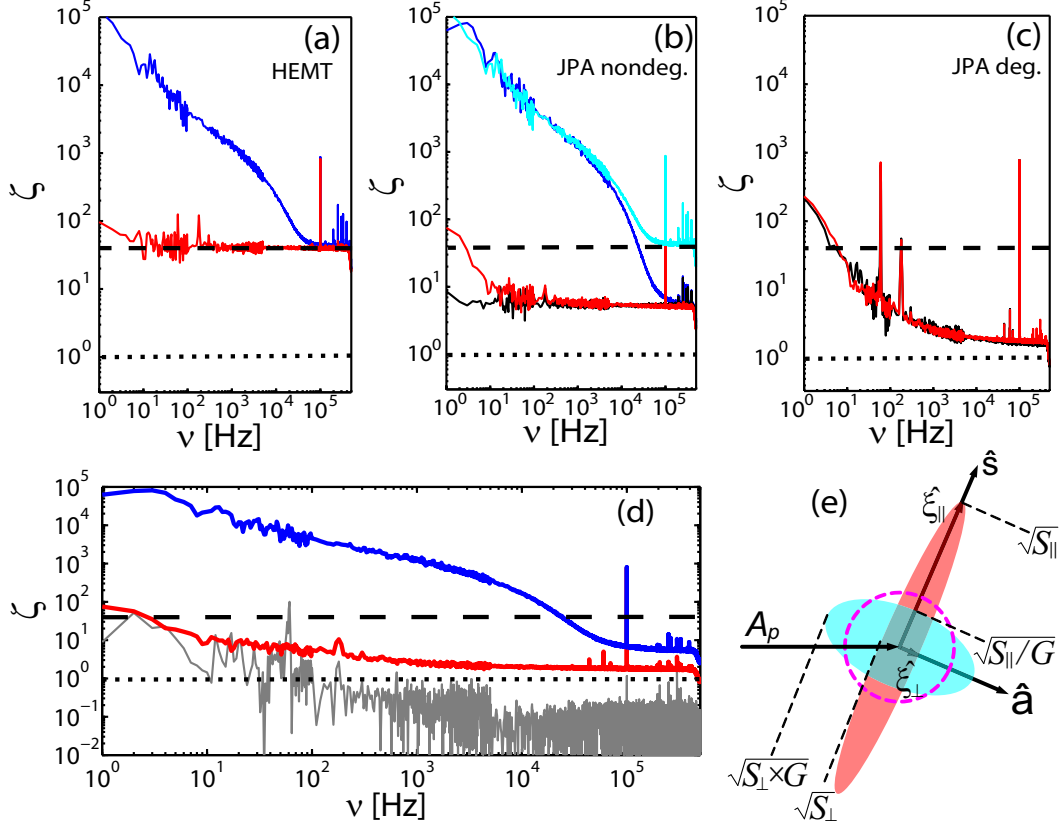


FIG. 4: Measured noise spectra  $S_{\parallel}$  (blue) and  $S_{\perp}$  (red), directly by HEMT (a), by JPA in non-degenerate mode (b) and JPA in degenerate mode ( $S_{\perp}$  only)(c). The HEMT noise floor (dashed line), the system noise floor—measured with  $A_e$  and  $A_s$  off—(solid black line), and the vacuum noise level (dotted line) are indicated in each subfigure. The lowest measured  $S_{\perp}$  (the minimum of the red lines in (a), (b), and (c)) is plotted by the red line in (d), which, after subtracting off the system noise floor (including HEMT, thermal and vacuum noise), yields the gray line. All the noise spectra are plotted in units of vacuum noise and are calculated by  $\zeta = S_{\xi}/(hf/4)$ , where  $S_{\xi}$  is the quadrature noise power spectral density(double-sided) in units of W/Hz measured at the output of IQ mixer expressed as apparent noise at the input of JPA. A calibration tone of known power,  $P_{\text{cal}} = -153.2$  dBm, is injected at the JPA input, allowing us to infer the gain of the amplification and mixing chain.  $P_{\text{cal}}$  is known, because the critical pump power  $P_c$  is accurately determined by a separate measurement performed in a liquid-helium test probe. In contrast to the ADR, for the test probe we are able to accurately calibrate the attenuation of the microwave cables carrying signals to the JPA[12]. The alignment of the resonator noise ellipse with the JPA amplification and squeezing quadratures are illustrated in (e). The input and output noise ellipses are shown in red and cyan, respectively. The HEMT noise is indicated by the pink dashed circle.